Development of the Subroutine Library 'UMMDp' for Anisotropic Yield Functions

Kai Oide*, Takaya Kobayashi*, and Hideo Takizawa**

*Mechanical Design & Analysis Corporation
Tokyo, Japan

**Nippon institute of technology
Saitama, Japan

Abstract: *To complement improvements in metal manufacturing technology, metal-forming simulations using advanced anisotropic yield functions are required in addition to common constitutive laws, especially in high-value-added application fields. Advanced finite element codes, such as Abaqus, enable application of anisotropic yield functions via user subroutines. However, such a technique requires securing human resources with professional skills and knowledge, and is not yet widely available. Over the last decade, the Japan Association for Nonlinear Computer Aided Engineering (JANCAE) has developed a subroutine library, including not only practically recognized anisotropic yield functions (e.g., Yoshida's 6th-order polynomial, Barlat's YLD2000-2d and YLD2004, Banabic's BBC2008, Cazacu's CPB2006, and Vegter's spline), but also subroutines that provide multi-port capability to any finite element codes to implement these yield functions. In the case of Abaqus, a framework for a UMAT subroutine is already prepared in the library as a common subroutine.*

The working group of JANCAE was launched from the idea of providing a multidisciplinary forum for steel researchers, design engineers, and software engineers through the medium of advanced finite element codes. The subroutine library is called the Unified Material Model Driver for Plasticity (UMMDp). This paper introduces the development of UMMDp and discusses a simulation of a drawing and redrawing process using some yield functions for its applications with Abaqus.

Keywords: *Anisotropic yield functions, Plasticity, Constitutive Model, Metal forming, JANCAE*

1. Introduction

With the spread of advanced finite element codes, it has become easy to simulate models that have non-linear materials. Particularly, in metal-forming problems, advanced anisotropic yield functions are required, and several yield functions have been proposed in the literature (Banabic 2010). However, application of these functions for simulations requires professional skills and knowledge, so these functions are not easily available for use.

The Japan Association for Nonlinear Computer Aided Engineering (JANCAE. President: Kenjiro Terada, Tohoku University), which is a non-profit organization (NPO JANCAE HP), has developed a subroutine library, over the last decade. The library includes practically recognized anisotropic yield functions (e.g., Yoshida's 6th-order polynomial (Yoshida 2013), Barlat's YLD2000-2d (Barlat 2003) and YLD2004 (Barlat 2005), Banabic's BBC2008 (Comsa 2008), Cazacu's CPB2006 (Cazacu 2006), and Vegter's spline (Vegter 2006)). Further, it contains the plug-ins to each available code, including Abaqus. In the working group of JANCAE, regardless of the respective positions and use codes, CAE engineers learn the basic theory of elasto-plasticity, develop subroutines of material models, and verify them on their finite element method (FEM) software. The main participants are volunteers from the working group and engineers for some software vendors. The subroutine library is called the Unified Material Model Driver for Plasticity (UMMDp) (Takizawa 2016).

The present paper describes the development of the user-subroutine library UMMDp for anisotropic yield functions and discusses some example simulations using some yield functions with Abaqus.

2. Stress integration and consistent tangent matrix

In a FE code, a material model is assembled in a stress integration as a constitutive equation. In the case of Abaqus, we can use UMAT for this. The roles of the material user-subroutines are identical for all FE codes. Further, the numerical procedures in the user-subroutines are independent of the kind of yield functions. Therefore, the stress integration method for arbitrary yield functions is summarized here.

In the backward Euler scheme, to evaluate the stress at increment $n+1$ for a given displacement, Jacobian $\partial\{\sigma\}/\partial\{\varepsilon\}$ at increment $n+1$ is used. The state in which the stress $\{\sigma_{n+1}\}$ is located on the isotropically hardened yield surface is described as

$$\sigma_e(\sigma_{n+1}) - \sigma_Y(p_{n+1}) = 0, \tag{1}$$

where σ_e is an arbitrary yield function, $p_{n+1} = p_n + \Delta p$ is the equivalent plastic strain, and $\sigma_Y(p)$ is the hardening function of p. By assuming the associated flow rule, the plastic strain increment $\{\Delta\varepsilon^p\}$ can be described as follows:

$$\{\Delta\varepsilon^p\} = \Delta p \frac{\partial\sigma_e}{\partial\{\sigma_{n+1}\}} \equiv \Delta p\{N_{n+1}\} \tag{2}$$

The direction of the plastic strain increment coincides with the outward normal to the yield surface of increment $n+1$. Here, $\{N\}$ is the 1st-order partial differential of σ_e with respect to the stress. If the elastic deformation is small enough, the additive decomposition of the total strain increment can be applied as $\{\Delta\varepsilon\} = \{\Delta\varepsilon^e\} + \{\Delta\varepsilon^p\}$. Thus, the updated stress can be written as

$$\begin{aligned}\{\sigma_{n+1}\} &= \{\sigma_n\} + [C^e]\{\Delta\varepsilon^e\} = \{\sigma_n\} + [C^e]\{\Delta\varepsilon\} - \Delta p[C^e]\{N_{n+1}\} \\ &\equiv \{\sigma^{tri}\} - \Delta p[C^e]\{N_{n+1}\},\end{aligned} \tag{3}$$

where $[C^e]$ is the matrix of Hooke's law, and $\{\sigma^{tri}\}$ is the stress, assuming that all the strains are elastic.

The stress increment $\{\Delta\sigma\} = \{\sigma_{n+1}\} - \{\sigma_n\}$ and equivalent plastic strain increment Δp are solved to satisfy Equations 1 and 3. First, the residual scalar g_1 and vector $\{g_2\}$ are defined as

$$g_1 = \sigma_e(\sigma_{n+1}) - \sigma_Y(p_n + \Delta p) \text{ and } \{g_2\} = \{\sigma_{n+1}\} - \{\sigma^{tri}\} + \Delta p[C^e]\{N_{n+1}\}, \tag{4}$$

respectively. These equations are linearized to obtain corrections $\{\delta\Delta\sigma\}$ and $\delta\Delta p$ by Newton–Raphson iteration, as follows:

$$g_1 + \{N\}^T\{\delta\Delta\sigma\} - \frac{\partial\sigma_Y}{\partial p}\{\delta\Delta p\} = 0, \quad \{g_2\} + [E]\{\delta\Delta\sigma\} + \delta\Delta p[C^e]\{N\} = 0, \tag{5}$$

where $[E] = [I] + \Delta p[C^e][\partial\{N\}/\partial\{\sigma\}^T]$ and $[I]$ is the unit matrix. Solving the above equations as simultaneous equations, $\delta\Delta p$ and $\{\delta\Delta\sigma\}$ can be obtained as

$$\delta\Delta p = \frac{g_1 - \{N\}^T[E]^{-1}\{g_2\}}{\{N\}^T[E]^{-1}[C^e]\{N\} + \partial\sigma_Y/\partial p} \text{ and } \{\delta\Delta\sigma\} = -[E]^{-1}\{\{g_2\} + \delta\Delta p[C^e]\{N\}\}. \tag{6}$$

The equations are updated iteratively with $\{\Delta\sigma\} + \{\delta\Delta\sigma\}$ and $\Delta p + \delta\Delta p$ until g_1 and $\{g_2\}$ converge.

The consistent tangent matrix that conforms to the algorithm can be obtained as the relationship between the perturbations of $\{\Delta\sigma\}$ and $\{\Delta\varepsilon\}$. The total differentials of Equations 1 and 3 are

$$\{N\}^T\{\delta\Delta\sigma\} - \frac{\partial\sigma_Y}{\partial p}\delta\Delta p = 0 \text{ and } \{\delta\Delta\sigma\} = [C^e]\{\delta\Delta\varepsilon\} - [C^e]\left\{\delta\Delta\{N\} + \Delta p\frac{\partial\{N\}}{\partial\{\sigma\}^T}\{\delta\Delta\sigma\}\right\}, \tag{7}$$

respectively. Using the above-mentioned $[E]$ and $[e] = [E]^{-1}[C^e]$, the relationship between the perturbations of $\{\delta\Delta\sigma\}$ and $\{\delta\Delta\varepsilon\}$ can be obtained as follows:

$$\{\delta\Delta\sigma\} = \left[[e] - [e]\{N\}\{N\}^T[e]\left(\{N\}^T[e]\{N\} + \frac{\partial\sigma_Y}{\partial p}\right)^{-1}\right]\{\delta\Delta\varepsilon\}$$

(8)

Thus, the updated stress and the consistent tangent matrix can be calculated only if the yield function σ_e and its 1st- and 2nd-order partial differentials, $\{N\}$ and $[\partial\{N\}/(\partial\{\sigma\}^T)]$, respectively, are given.

3. Framework of the UMMDp subroutine library

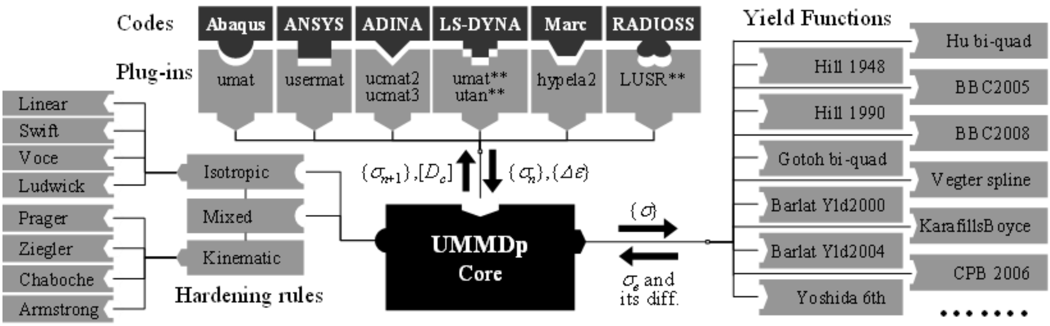

Figure 1. Framework of UMMDp.

As mentioned above, the material model can be unified as a common numerical procedure, externalizing the variety of FE codes and yield functions.

Figure 1 shows the framework of the UMMDp. The core that executes the common numerical procedure is called from the user-subroutines of FE codes. Each user-subroutine acts as a plug-in, which connects the UMMDp core to the FE codes. In the right branch, various yield functions are modularized as subroutines, in which σ_e and its differentiations are calculated as the arguments. Various yield functions have been implemented in the UMMDp, such as Hill's 1948 (Hill 1948) and 1990 (Hill 1990), Gotoh's bi-quadratic (2D) (Gotoh 1977), Hu's bi-quadratic (3D) (Hu 2005), Yoshida's 6th-order polynomial (Yoshida 2013), Barlat's YLD89 (Barlat 1989), YLD2000-2d (Barlat 2003), and YLD2004 (Barlat 2005), Banabic's BBC2005(Banabic 2008) and BBC2008 (Comsa 2008), Cazacu's CPB2006 (Cazacu 2006), Karafillis-Boyce (Karafillis 2008), and Vegter's spline (Vegter 2006). If only the parameters for each model are prepared, any function can be used. Furthermore, as shown in the left branch, various hardening rules, including kinematic hardening, are modularized for future expansion.

4. Wrinkling during cup drawing

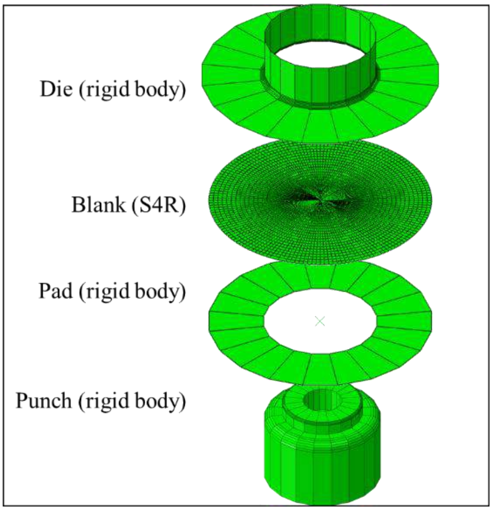

Figure 2. A drawing operation model for wrinkling.

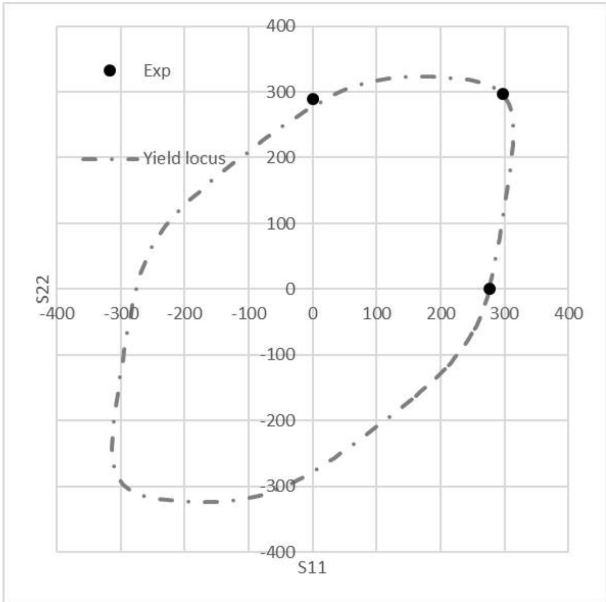

Figure 3. Yield locus with experimental plots for wrinkling.

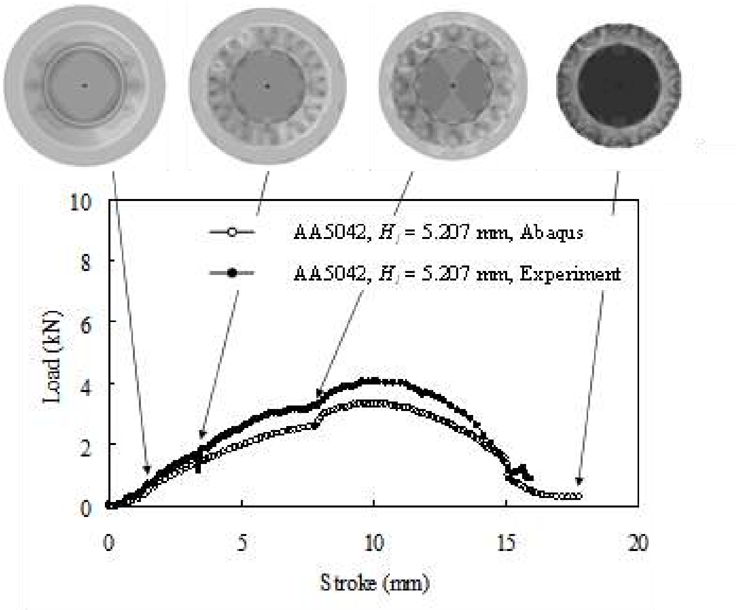

Figure 4. Load–stroke diagram during the drawing process.

The first example shows wrinkling during cup drawing of the aluminum sheet using the UMMDp. Figure 2 shows the drawing operation model (Dick 2014). YLD2000 (Barlat 2003) parameters in NUMISHEET2014 BM4 (Dick 2014) are used in the simulations, and Figure 3 shows the yield locus together with the experimental plots, in which S11 and S22 represent the stress in the rolling direction and the transverse direction, respectively. The yield locus agrees with the experimental results.

Figure 4 shows the load–stroke diagram during the drawing process using Abaqus with UMMDp. The result is similar to the experimental result, and the wrinkling can be recognized.

5. A drawing and redrawing operation

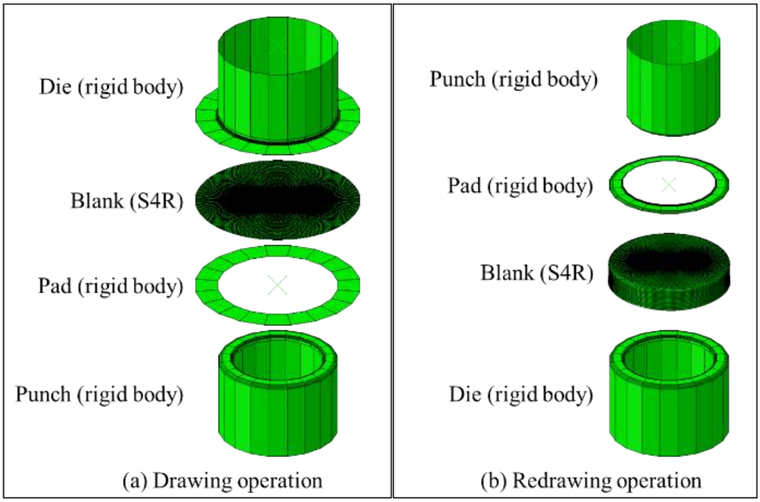

Figure 5. A drawing and redrawing operation model.

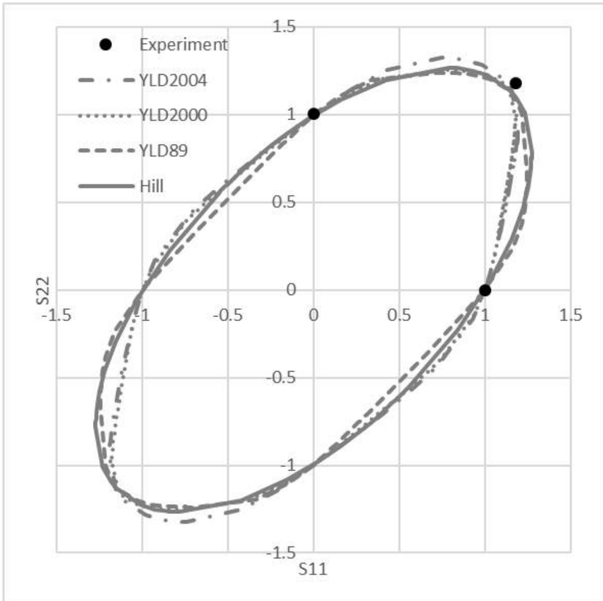

Figure 6. Yield loci with experimental plots.

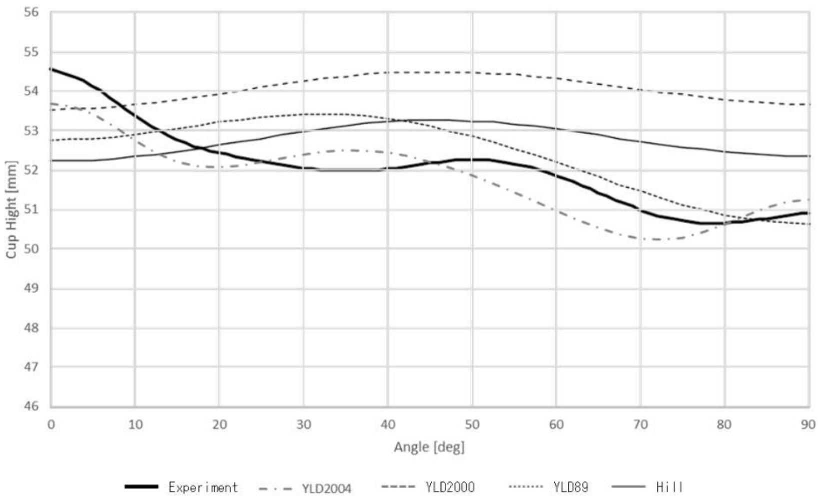

Figure 7. The cup height.

As a second example, FEA for a drawing and redrawing process of the aluminum sheet is performed using the UMMDp. Figure 5 shows the drawing and redrawing operation model (Watson 2016). Four yield functions YLD2004 (Barlat 2005), YLD2000 (Barlat 2003), YLD89 (Barlat 1989), and Hill's 1948 (Hill 1948) are used in the simulations. Figure 6 shows the yield loci by using the parameters in NUMISHEET2016 BM1 (Watson 2016) together with the experimental plots. The yield loci of all functions agree with the experimental results. YLD89 and Hill's 1948 are similar, but YLD2004 and YLD2000 are slightly different from them.

Figure 7 shows the cup height after redrawing of FEA performed using Abaqus in conjunction with four yield functions of UMMDp. The phase of cup height of YLD89 and Hill's 1948 are similar, and YLD2000 is also similar to these two, although it is different in size. YLD2004 has a reverse phase compared to the other three, and it is almost similar to the experimental result.

6. Conclusion

A universal user-subroutine library for various anisotropic yield functions was developed. This library is available for major FE codes including Abaqus and enables users to easily implement their yield functions. By applying this to two drawing operations, we have obtained different results for some anisotropic yield functions.

7. Acknowledgments

All programs were developed by participants of the Material Modeling Working Group of the Japan Association for Nonlinear CAE (JANCAE). The authors would like to thank everyone who supported the present project.

8. References

1. Banabic D., Barlat F., Cazacu O. and Kuwabara T., “Advances in anisotropy and formability,” Int. J. Mater. Form. 3, 165, 2010.

2. Non-profit organization Japan Association for Nonlinear CAE, HP: http://www.jancae.org/index.html.

3. Yoshida F., Hamasaki H. and Uemori T., “A user-friendly 3D yield function to describe anisotropy of steel sheets,” Int. J. Plasticity 45, 119, 2013.

4. Barlat F., Brem J. C., Yoon J. W., Chung K., Dick R. E., Lege D. J., Pourboghrat F., Choi S. H. and Chu E., “Plane stress yield function for aluminum alloy sheets – part 1: theory,” Int. J. Plasticity 19, 1297, 2003.

5. Barlat F., Aretz H., Yoon J. W., Karabin M. E., Brem J. C. and Dick R. E., “Linear transformation – based anisotropic yield functions,” Int. J. Plasticity 21, 1009, 2005.

6. Comsa D. S. and Banabic D., “Plane-stress yield criterion for highly-anisotropic sheet metals,” 7th Int. Conf. NUMISHEET 2008.

7. Cazacu O., Plunkett B. and Barlat F., “Orthotropic yield criterion for hexagonal closed packed metals,” Int. J. Plasticity 22, 1171, 2006.

8. Takizawa H., Kuwabara T., Oide K., Yoshida J., “Development of the subroutines library ‘UMMDp’ for anisotropic yield functions commonly applicable to commercial FEM codes,” J. Physics: Conference Series, 734, 032028, 2016.

9. Vegter H. and Boogaard A. H., “A plane stress yield function for anisotropic sheet material by interpolation of biaxial stress states,” Int. J. Plasticity 22, 557, 2006.

10. Hill R., “A theory of the yielding and plastic flow of anisotropic metals,” Proc. Royal Society of London, Series A, Mathematical and Physical Sciences, 193, 1033, 281, 1948.

11. Hill R., “Constitutive modelling of orthotropic plasticity in sheet metals,” J. Mech. Phys. Solids, 38, 3, 405, 1990.

12. Gotoh M., “A theory of plastic anisotropy based on a yield function of forth order (plane stress state) – I,” Int. J. mech. Sci. 19, 505, 1977.

13. Hu W., “An orthotropic yield criterion in a 3-D general stress state,” Int. J. Plasticity, 21, 1771, 2005.

14. Barlat F. and Lian J., “Plastic behavior and stretchability of sheet metals. part I: a yield function for orthotropic sheets under plane stress conditions,” Int. J. Plasticity, 5, 51, 1989.

15. Banabic D., Comsa D. S., Sester M., Selig M., Kubli W., Mattiasson K. and Sigvant M., “Influence of constitutive equations on the accuracy of prediction in sheet metal forming simulation,” Numisheet 2008.

16. Karafillis A. P. and Boyce M. C., “A general anisotropic yield criterion using bounds and a transformation weighting tensor,” J. Mech. Phys. Solids, 41, 12, 1859, 1993.

17. Dick, R., Cardoso, R., Yoon, J.W. and Paulino, M., 2014, Benchmark 4, The 9th International Conference and Workshop on Numerical Simulation of 3D Sheet Metal Forming Processes (NUMISHEET2014), Melbourne, http://www.numisheet2014.org/, 2014.

18. Watson M., Dick R., Huang Y. H., Lockley A., Cardoso R. and Santos A., “Numisheet 2016 Benchmark 1 – Failure Prediction after Cup Drawing, Reverse Redrawing and Expansion,” J. Physics: Conference Series 734 022001, 2016.